Physica B 185 (1993) 325–331
North-Holland

PHYSICA B

Electronic structure and dynamical behaviour of different bound-exciton complexes in ZnSe bulk crystals

G.H. Kudlek, U.W. Pohl, Ch. Fricke, R. Heitz, A. Hoffmann, J. Gutowski[1] and I. Broser

Institut für Festkörperphysik, Technische Universität Berlin, Germany

High-quality ZnSe crystals grown by the high-pressure Bridgman method show emissions of the free exciton (X) in the excitonic energy range as well as bound exciton lines I_1 and I_2. The I_{2i}-lines, which are observed in excitation spectra of the (D^0, X)-complex, are explained taking into account a three-particle model with excited $|n, l\rangle$ hole states for the (D^0, X)-complex. Otherwise the (A^0, X) ground state is split by the (j, j)-coupling of the two Γ_8-holes into two separate levels. From time-resolved luminescence the specified rise and decay times of different bound excitons complexes are determined.

1. Introduction

ZnSe is a highly interesting II–VI compound for application in optical or electro-optical devices. The production of such components requires low-resistivity p- and n-type ZnSe. Successful doping of ZnSe with both kinds of dopants was recently demonstrated with MBE-grown structures [1].

The process of impurity incorporation, however, is not well understood. In addition, the impurity-related exciton spectra, which usually are recorded to judge on the doping efficiency and the crystal quality, are not understood in detail. We therefore studied the electronic structure and dynamical behaviour of free and different bound-exciton complexes in ZnSe crystals. To exclude the influence of strain occurring in heterostructures [2] we used unstrained ZnSe bulk crystals.

Correspondence to: G.H. Kudlek, Institut für Festkörperphysik, Technische Universität Berlin, Hardenbergstrasse 36, D-1000 Berlin 12, Germany.
[1] Now at Institut für Experimentelle Physik, Universität Bremen, D-2800 Bremen 33.

2. Experimental

The ZnSe samples were prepared by the vertical high-pressure Bridgman method from a stochiometric melt.

For luminescence and excitation spectroscopy a pulsed dye laser (spectral line width 0.02 nm) pumped by an excimer laser (Lambda Physik) was used.

For the time-resolved measurements we used an actively mode-locked Nd: YAG laser (Coherent) with a frequency-tripling BBO crystal pumping a dye laser. The photoluminescence signal was analysed by a single-photon-counting system and a micro-channel-plate photomultiplier tube.

3. Results and discussion

As a basis of our optical investigations, we recorded the photoluminescence under band-to-band excitation. Figure 1 shows the luminescence spectrum of an undoped ZnSe crystal in the excitonic energy regime. Dominant features are the free exciton X, several lines denoted I_{2i} as recombinations from different excited states of

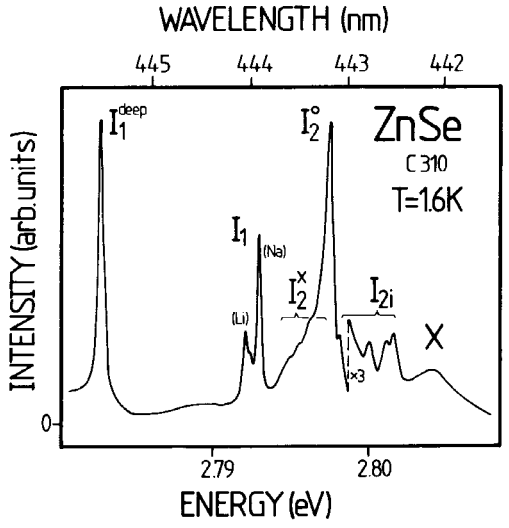

Fig. 1. Luminescence spectrum of an undoped cubic ZnSe crystal in the excitonic energy range.

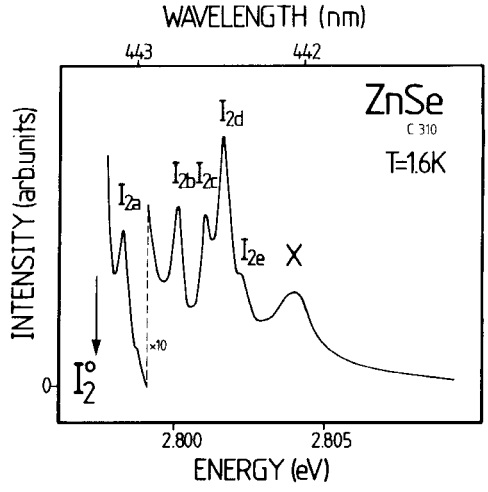

Fig. 2. Excitation spectrum of the I_2^0 line (for explanation see text).

the (D^0, X) complex, and some I_{2^x} lines being recombinations of different donor-bound excitons in their electronic ground states. Additionally, three emission lines I_1^{Li}, I_1^{Na} and I_1^{deep} are observed, which are assigned to excitons bound to various acceptors of different chemical nature. For lower energies (not depicted in this figure) two series of dominant donor–acceptor-pair recombinations are detected, which are correlated to the energy levels of the Li and Na acceptors.

3.1. Electronic structure

In the following chapter we will discuss the electronic structure of differently bound excitons in not intentionally doped bulk ZnSe. We distinguish between donor-bound exciton complexes (D^0, X) and acceptor-bound exciton complexes (A^0, X).

(D^0, X) complexes

For a better spectral separation of the I_{2i}-lines we carried out an excitation spectrum of the dominant I_2^0 transition (see fig. 2). Besides a resonance dip in the energy region of the free exciton at 2.80315 eV five separated transitions $I_{2a,b,c,d,e}$ could be resolved, exhibiting energy distances between 0.82 meV and 4.70 meV with respect to I_2^0.

Similar transitions have already been reported by Dean et al. [3], Merz et al. [4] and Isshiki et al. [5] to occur in the excitation spectra of differently donor-doped ZnSe crystals. The origin of these excited states of the (D^0, X)-complexes, however, has not been clarified in a satisfying way. We will demonstrate that the I_{2i} resonances can be well understood in terms of excited single-hole states. Since the excited states of the electron are shifted against the ground state by about 3/4 of the donor Rydberg energy E_D, they can be excluded as an explanation for levels involved in the I_{2i} transitions. The only explanation of these transitions can therefore be given taking into account several excited hole states. The proposed model which was initially used in molecular physics has already been applied successfully for donor–exciton complexes in InP [6] and for excited states of donor-bound excitons in wurtzite-type semiconductors [7]. The electron–electron and electron–hole correlations are neglected in the model since only the energy separation of the exited states are of interest. Using this approximation, the three-particle Schrödinger equation of the (D^0, X) complex can be written as

$$\left|2E_g - \frac{\hbar^2}{2m_e}(\Delta r_{e1} + \Delta r_{e2}) - \frac{\hbar^2}{2m_h}\Delta r_h + V(r_{e1}, r_{e2}, r_h)\right|\Psi(r_{e1}, r_{e2}, r_h) = E\Psi(r_{e1}, r_{e2}, r_h) \quad (1)$$

with the coordinates r_{e1}, r_{e2} of the two involved electrons, and r_h that of the hole of this complex. The wavefunction of the (D^0, X) complex is described as a product of one-particle states

$$\Psi(r_{e1}, r_{e2}, r_h) = \Phi(r_{e1})\Phi(r_{e2})\Phi(r_h)\,. \quad (2)$$

Using the separation of the Schrödinger equation we obtain the following one-particle eigenvalue equation for the single hole:

$$\left[-\frac{\hbar^2}{2m_h}\Delta r_h + V(r_h)\right]\Phi(r_h) = \varepsilon_h\Phi(r_h) \quad (3)$$

with the potential

$$V(r_h) = -\frac{e^2}{\varepsilon_0 r_h}\left[1 - 2\,e^{r_h/a_e} + \frac{r_h}{a_e}\right] \quad (4)$$

with the radius r_h of the hole with respect to the impurity center, and a_e that of the electron of the donor. To solve the eigenvalue equation (3), $V(r_h)$ can be approximated by a suitable model potential, known as the Kratzer potential [8]:

$$V(r_h) = -2D\left(\frac{b}{r_h} - \frac{b^2}{2r_h^2}\right) \quad (5)$$

with the parameters s and t and $D = se^2/(\varepsilon_0 a_e)$ and $b = ta_e$.

The fit of the Kratzer potential to the real potential $V(r_h)$ yields the parameters $s = 1.0136$ and $t = 1.337$. Using this potential we could solve eq. (3) and obtain total energy levels of the (D^0, X) complex (eq. (6)), for which the hole is in one of its excited states $|n, l\rangle$ (with n its radial and l its angular momentum quantum number). The electrons remain in their single-particle ground state. We have

$$E|n, l\rangle = 2E_g + 2E_D\left\{\left(\frac{a_D}{a_e}\right)^2 - \frac{11}{8}\frac{a_D}{a_e} - \frac{s^2t^2}{2}\frac{m_e}{m_h} \times \left(n + \frac{1}{2} + \sqrt{\left(l + \frac{1}{2}\right)^2 + \frac{st^2 a_e}{a_D}\frac{m_e}{m_h}}\right)^{-2}\right\}. \quad (6)$$

E_g is the bandgap, a_D the donor Bohr radius. For the calculations of the $|n, l\rangle$ states we used a donor Rydberg energy E_D of 26 meV which corresponds well to the binding energy value of 5.6 meV of the (D^0, X) complex taken from the literature [9]. Taking into account a ratio of the effective masses $\sigma = m_e/m_h$ of 0.24 we obtain a ratio $a_D/a_e = 0.38$, which strongly depends on σ. With this value the relative distances of the excited states $E|n, l\rangle$ with respect to the ground state $E|0, 0\rangle$ can be determined. The computed distances and the experimentally observed energy spacings of the I_{2i} resonances to I_2^0 are presented in table 1. For all transitions the calculated $E|n, l\rangle - E|0, 0\rangle$ values agree very well with the energy distances $E(I_{2i}) - E(I_2^0)$. Therefore, all I_{2i}-lines are assigned to definite excited single-hole states with quantum numbers $|n, l\rangle$.

The energy values of the $|n, l\rangle$ states are sensitively depending on the σ ratio, which has been verified in strained ZnSe/GaAs heterolayers [2], and on the donor Rydberg energy E_D. As a test of the used model we look at the I_{2i} transitions of Al-, Cl- and Ga-doped ZnSe crystals (table 2) which were observed by Isshiki et al. [5]. By adjusting E_D to the chemically different (D^0, X) complexes and using eq. (6) we calculated the energies of the first five

Table 1
Comparison of the calculated energy distances between the $|n, l\rangle$-states and the $|0, 0\rangle$ ground state, and the experiment observed $E(I_{2i}) - E(I_2^0)$ values.

Line	$\|n, l\rangle$	Energy I_{2i} (eV)	ΔE_{exp} (meV)	ΔE_{cal} (meV)
I_2^0	0, 0	2.79753	–	–
I_{2a}	0, 1	2.79835	0.82	0.81
I_{2b}	1, 0	2.80014	2.61	2.82
I_{2c}	1, 1	2.80107	3.54	3.29
I_{2d}	2, 0	2.80165	4.12	4.48
I_{2e}	2, 1	2.80223	4.70	4.77
X	–	2.80315	5.62	–

Table 2
Application of the used model to determine the energy spacings between the $|n, l\rangle$-states and the $|0, 0\rangle$ ground state in differently donor-doped ZnSe crystal. The experimental datas are taken from Isshiki et al. [5].

Line	$\|n, l\rangle$	ZnSe : Al E_D = 25.6 meV		ZnSe : Cl E_D = 26.1 meV		ZnSe : Ga E_D = 27.2 meV	
		ΔE_{exp} (meV)	ΔE_{cal} (meV)	ΔE_{exp} (meV)	ΔE_{cal} (meV)	ΔE_{exp} (meV)	ΔE_{cal} (meV)
I_{2a}	0, 1	0.64	0.79	0.68	0.81	0.82	0.85
I_{2b}	1, 0	2.46	2.77	2.46	2.83	2.80	2.95
I_{2c}	1, 1	3.30	3.24	3.44	3.30	3.81	3.44
I_{2d}	2, 0	3.58	4.41	3.72	4.49	4.11	4.68
I_{2e}	2, 1	3.96	4.69	4.08	4.78	4.48	4.99

excited $|n, l\rangle$ states which correspond well to the measured values.

Summarized, the investigation of the I_{2i} lines is a suitable tool to determine the chemical nature of the involved neutral donor in specific (D^0, X) complexes.

(A^0, X) complexes

In the luminescence spectrum (see fig. 1) three I_1 emission lines of different acceptor–exciton complexes were detected. The incorporation of Li and Na into the crystal results in two I_1 lines near 2.972 eV. Additionally, a recombination of a more deeply bound acceptor–exciton complex I_1^{deep} was observed at 2.782 eV.

To determine the electronic structure of a single (A^0, X) complex, and to avoid a superposition of several I_1 lines, we used for these investigations a Na-doped cubic ZnSe sample. We observe a further sharp line $I_1'^{Na}$ on the higher-energy side of the I_1^{Na} which becomes stronger with increasing temperatures (see insert of fig. 3). At a temperature of 8 K, the intensities of I_1^{Na} and $I_1'^{Na}$ are equal. From this thermalization behaviour and the energy spacing of 1.1 meV we calculated the oscillatory strength ratio $I_1^{Na} : I_1'^{Na}$ to be approximately 1:5.

Figure 3 shows the comparative excitation spectra of the I_1^{Na} line and the $I_1'^{Na}$ line. The I_1^{Na} excitation spectrum exhibits a strong $I_1'^{Na}$ resonance at the same energy as the corresponding luminescence line. Additionally, a dip at the free-exciton energy and weaker resonance at the

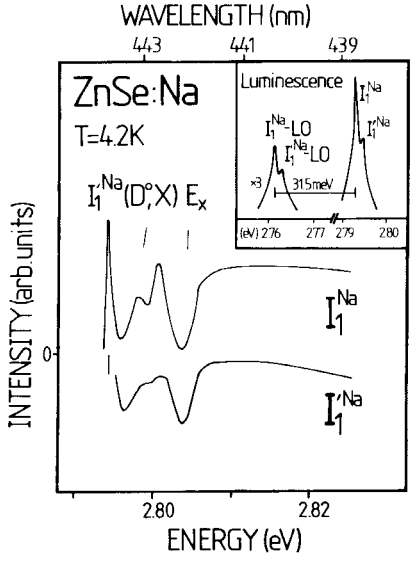

Fig. 3. Comparative excitation spectra of the I_1^{Na} and $I_1'^{Na}$ luminescence lines. The insert shows the respective luminescence spectrum at 4.2 K.

(D^0, X) transition energies are observed. The spectrum of the $I_1'^{Na}$ also shows a dip at the free-exciton energy and the resonances in the (D^0, X) energy range.

Due to the strong correlation between I_1^{Na} and $I_1'^{Na}$, it is evident that both lines belong to transitions of the same (A^0, X) complex. In the following discussion the index 'Na' is omitted because the phenomena reflect the general nature of acceptor-bound excitons in zinc-blende structured semiconductors. An explanation of I_1 and I_1' could be given in terms of a fine-structure

splitting of the (A^0, X) electronic ground state. For (A^0, X) complexes in zinc-blende compounds the two Γ_8^v holes, one originating from the neutral acceptor and the other from the free exciton, couple to give combinations of antisymmetric wavefunctions, yielding a total hole momentum of $J_h = 0$ and $J_h = 2$. The additional coupling of the Γ_6 electron leads to three different states with Γ_6 ($J = 1/2$), Γ_8 ($J = 3/2$) and $\Gamma_7 + \Gamma_8$ ($J = 5/2$) symmetry. The Γ_8 and $\Gamma_7 + \Gamma_8$ states are separated by the cubic-crystal field, whereas the $\Gamma_7 + \Gamma_8$ degeneracy can be lifted by the electron–hole interaction.

The observed splitting into the $J_h = 0$ and $J_h = 2$ states is a consequence of the dominating hole–hole interaction ((j, j)-coupling). Our experimental results can be explained by such a fine-structure of the (A^0, X) ground state, split by (j, j)-coupling. A further splitting of the $J_h = 0$ term could not be resolved.

The theoretical oscillator strength ratio for unthermalized transitions from the acceptor ground state into the level related to $J_h = 0$ and $J_h = 2$ is 1:5 [11] and agrees very well with the observed ratio in the above-described temperature-dependent measurements of I_1 and I_1'.

Therefore, the $J_h = 2$ related term, which is correlated with the I_1' transition, is supposed to represent the upper level. A similar situation was found for the (Li^0, X) complex, whereas an analogous specific $I_1^{'deep}$ transition was not observed in the excitation spectrum of the I_1^{deep} line. The structure of the latter center thus obviously deviates from that discussed above.

Respective models of the (A^0, X) complex were successfully applied to other zinc-blende compounds, like ZnS [12], InP [13], GaAs [14] and Si [15].

3.2. Dynamical behaviour

In fig. 4 the transients of the free and different bound-exciton emissions are shown. All rise and decay times of these exciton emissions lie in the ps time range. With increasing binding energies an increase of the lifetimes was detected. For the analysis of the observed luminescence transients we used a sum of two exponential functions to fit

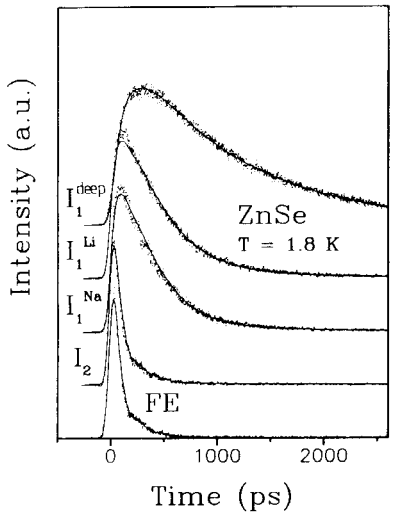

Fig. 4. Transients of the free-exciton and different bound-exciton emissions. The time-integrated photoluminescence spectrum of this sample is depicted in fig. 1.

the formation time τ_r and the decay time τ_d. The obtained τ_d times are summarized for different exciton emissions in the table 3.

To calculate the lifetimes of differently bound excitons we used the formula of Rashba and Gurgenishvili [16]. The authors introduced a model relating the enhanced oscillator strengths of the bound excitons f_{BE} to those of the free exciton f_{FE}:

$$f_{BE} = \frac{8\pi a_{BE}^3}{V} f_{FE} . \tag{7}$$

In this model the oscillator strength of the bound excitons f_{BE} is proportional to the Bohr radius a_{BE} of the bound exciton and the volume V of a primitive elementar cell. The wavefunction of the bound exciton is derived from the effective-mass theory considering the interaction with the

Table 3
Calculated lifetimes, using eqs. (10) and (11), and measured lifetimes of differently bound excitons.

Line	I_2	I_1^{Na}	I_1^{Li}	I_1^{deep}
E_B (meV)	5.6	10.0	10.8	20.2
τ^{cal} (ps)	31	294	329	842
τ^{exp} (ps)	40	280	350	1020

neutral impurity as a delta-function potential. The amplitude of this model potential is adjusted to the binding energy of the involved complex.

Since a_{BE} is given by

$$a_{BE} = \frac{\hbar}{\sqrt{2m_{ex}E_B}}, \tag{8}$$

with

$$m_{ex} = m_h + m_e, \tag{9}$$

the lifetime τ_d which is given by

$$\tau_d = \frac{4.5\lambda^2}{nf_{BE}} \tag{10}$$

is a function of the binding energy. λ is the emitted-light wavelength and n the refractive index.

Using $n = 2.61$, $m_{ex} = 0.81m_0$ and $V = 4.1 \times 10^{-2}$ nm^3 [17] we calculated the lifetimes of different (A^0, X) complexes. These values are given in the second row of table 3 and agree very well with the measured lifetimes.

When we used the model of Rashba and Gurgenishvili for the calculation of the I_2 decay time we obtained a value which is four times larger than the experimental ones. This contradiction could be solved taking into account that the potential of the (D^0, X) complex deviates considerably from a simple delta function which could be used in the previously discussed case of the (A^0, X) complexes. For (D^0, X) complexes a Morse potential [18] was found to be a suitable model potential. To determine the lifetime of the I_2 we used the model of Sanders and Chang [18]. They described the ratio of the oscillator strength of (A^0, X) and (D^0, X) complexes with identical binding energies.

The oscillator strength ratio depends on integral $\langle I | F \rangle^2$ between initial (I) and final (F) state, which is strongly sensitive to σ. We have

$$f_{BE} \sim \frac{P^2}{\hbar\omega} |\langle I|F\rangle|^2 . \tag{11}$$

Here P describes the optical matrix element between the Bloch states of the conduction band minimum and the valence band maximum.

Using the value $\sigma = 0.24$ (see section 3.1) we obtain a considerably larger $f_{(D^0,X)}$ value in comparison with the respective $f_{(A^0,X)}$-value. Regarding this behaviour we obtain from eqs. (7) and (11) a decay time of 31 ps for a (D^0, X) complex with a binding energy of 5.6 meV, which corresponds well with the measured value.

Additionally, these time-dependent measurements demonstrate that exciton capture at impurities is a dominant mechanism which lowers the free-exciton concentration within the first few tens ps.

4. Conclusion

We determined the term structure of (D^0, X) and (A^0, X) complexes in zinc-blende ZnSe bulk crystals. The (D^0, X) complex exhibits several excited single-hole states with quantum numbers $|n, l\rangle$. The ground state of the (A^0, X) complex is separated by the hole–hole interaction into two terms.

The investigation of these excited states made it possible to indicate the chemical nature of the incorporated shallow impurities.

The oscillator strength and the binding energy of the involved bound excitons could be determined by time-resolved measurements.

Acknowledgement

This work was supported by the 'Deutsche Forschungsgemeinschaft'.

References

[1] M.A. Haase, J. Qiu, J.M. DePuydt and H. Cheng, J. Appl. Phys. 59 (1991) 1272.

[2] G. Kudlek, N. Presser, U.W. Pohl, J. Gutowski, J. Lilja, E. Kuusisto, K. Imai, M. Pessa, K. Hingerl, E. Abramof, A. Pesek, H. Pauli and H. Sitter, J. Cryst. Growth 117 (1992) 309.

[3] P.J. Dean, D.C. Herbert, C.J. Werkhoven, B.J. Fitzpatrick and R.N. Bhargava, Phys. Rev. B 23 (1981) 4888.
[4] J.L. Merz, H. Kukimoto, K. Nassau and J. Shiever, Phys. Rev. B 6 (1972) 545.
[5] M. Isshiki, T. Kyotani, K. Masumoto, W. Uchida and S. Suto, Phys. Rev. B 36 (1987) 2568.
[6] A.M. White, P.J. Dean and B. Day, J. Phys. C 7 (1974) 1400.
[7] J. Puls, F. Henneberger and J. Voigt, Phys. Stat. Sol. B 119 (1983) 291.
[8] J. Puls, Thesis, Humboldt University, Berlin 1982.
[9] Landolt–Börnstein, ed. O. Madelung, (Springer-Verlag, Berlin, 1982).
[10] W. Ungier, M. Suffczynski and J. Adamowski, Phys. Rev. B 24 (1981) 2109.
[11] A.M. White, J. Phys. C 6 (1973) 1971.
[12] J. Gutowski, I. Broser and G. Kudlek, Phys. Rev. B 39 (1989) 3670.
[13] H. Mathieu, J. Chamassel and F.B. Chekroun, Phys. Rev. B 29 (1984) 3438.
[14] W. Schairer, D. Bimberg, W. Kottler, K. Cho and M. Schmidt, Phys. Rev. B 13 (1976) 3452.
[15] K.R. Elliott, G.C. Osbourn, D.L. Smith and T.C. McGill, Phys. Rev. B 17 (1978) 1808.
[16] E.I. Rashba and G.E. Gurgenishvili, Sov. Phys. Solid State 4 (1962) 759.
[17] T. Steiner, M.L. Thewalt and R.N. Bhargava, Solid State Commun. 56 (1985) 933.
[18] G.D. Sanders and Y. Chang, Phys. Rev. B 28 (1983) 5887.